Towards a compact, high-speed optical linkbased 3D optoacoustic imager

Ozsoy, Cagla ; Cossettini, Andrea ; Hager, Pascal ; Vostrikov, Sergei ; Luis Dean-Ben, Xose ; Benini, Luca ; Razansky, Daniel

Abstract: We demonstrate the feasibility of a compact real-time 3D optoacoustic (OA) imager employing a novel low-cost software-defined ultrasound digital acquisition platform. It supports simultaneous signal acquisition from up to 192 ultrasound channels and a direct optical link (2x 100G Ethernet) to the host-PC for high-frame-rate image acquisitions. Real-time 3D imaging experiments with light-absorbing phantoms and the wrist of a healthy volunteer are reported. These results pave the way toward a new generation of compact, affordable, and flexible hand-held OA scanners.

DOI: https://doi.org/10.1109/sensors47125.2020.9278772

Towards a compact, high-speed optical link-based 3D optoacoustic imager

Çağla Özsoy[1], Andrea Cossettini[2], Pascal Hager[2], Sergei Vostrikov[2], Xosé Luís Deán-Ben[1], Luca Benini[2,3], and Daniel Razansky[1]

[1]Institute for Biomedical Engineering and Institute of Pharmacology and Toxicology, University of Zurich and ETH Zurich, Switzerland
[2]Integrated Systems Laboratory, ETH Zurich, Switzerland
[3]Department of Electrical, Electronic, and Information Engineering, University of Bologna, Italy

***Abstract*—We demonstrate the feasibility of a compact real-time 3D optoacoustic (OA) imager employing a novel low-cost software-defined ultrasound digital acquisition platform. It supports simultaneous signal acquisition from up to 192 ultrasound channels and a direct optical link (2x 100G Ethernet) to the host-PC for high-frame-rate image acquisitions. Real-time 3D imaging experiments with light-absorbing phantoms and the wrist of a healthy volunteer are reported. These results pave the way toward a new generation of compact, affordable, and flexible hand-held OA scanners.**

Keywords—3D imaging; optoacoustic; ultrasound

I. Introduction

Despite the long history and wide use of pulse-echo ultrasound (US) in the clinical setting, this modality is continuously being advanced with new developments emerging in both hardware and software [1]. Particularly, digital US imaging systems providing analog-to-digital conversion and partial processing at the probe have facilitated the implementation of new imaging approaches as well as reducing size, complexity, and cost by avoiding the expensive and bulky cables of analog probes and enabling the usage of standard workstations, with no US-specific hardware, connected to the digital probe [2,3]. In addition to traditional pulse-echo US, optoacoustic (OA) imaging and tomography have emerged in the last decade and are gaining maturity as a preclinical imaging tool [4,5]. More recently, hand-held scanners specifically adapted to this modality have been used in clinical trials [6,7], offering promising prospects for its eventual clinical translation. Likewise, vast efforts have also been directed towards the integration of OA and US scanners [8,9,10]. Existing embodiments, however, rely on expensive lasers and complex acquisition systems not integrated into the probe. The clinical translation of the OA technology can then be significantly fostered with new developments in hardware components enabling the implementation of more compact and affordable scanners.

OA technology is characterized by a wide range of embodiments tailored to specific applications [4]. Being a relatively recent development in the biomedical imaging pantheon, OA hardware and software components have not been fully optimized. In particular, signal digitization generally relies on expensive and bulky digital acquisition systems [11,12], which hamper the development of more affordable and compact systems better suited for clinical applications. Yet, fundamental differences between US and OA must be taken into account for the optimal design of the acquisition electronics. In particular, OA tomographic imaging operates in a pure detection mode by recording very weak OA responses with orders of magnitude lower pressures compared to diagnostic US (often sub-Pascal levels). On the other hand, no compounding is involved in OA image formation. Thus, in principle, full 3D tomographic information can be acquired with a single excitation laser pulse that only lasts a few nanoseconds. This unique capability of the OA method has been exploited for ultrafast imaging at kilohertz volumetric frame rates with the digital data throughput capacity remaining the main bottleneck [13].

In this work, we introduced a compact high-speed three-dimensional (3D) OA imager based on a novel US digital acquisition architecture. Experiments are performed up to 100 frames per second, where the speed is limited by the laser pulse frequency. OA imaging of light-absorbing microspheres and human vasculature demonstrate the feasibility of OA imaging with a low-cost (3.000 US dollars) and small-form-factor system.

II. Materials and Methods

A. Optoacoustic Imaging System

Fig. 1 shows the OA imaging setup used in this work. OA responses are generated by a wavelength-tunable (690-900nm, tuned to 800nm in the experiments) optical parametric oscillator (OPO) laser source (InnoLas Laser GmbH, Krailling, Germany) emitting short laser pulses (<10 ns duration) with a pulse repetition frequency (PRF) up to 200 Hz. The light beam is guided via a custom-made silica fused-end fiber bundle (CeramOptics GmbH, Bonn, Germany) to illuminate the imaged object. The per-pulse energy delivered to the skin surface was kept below 20mJ while the illumination beam width is approximately 10 mm, thus

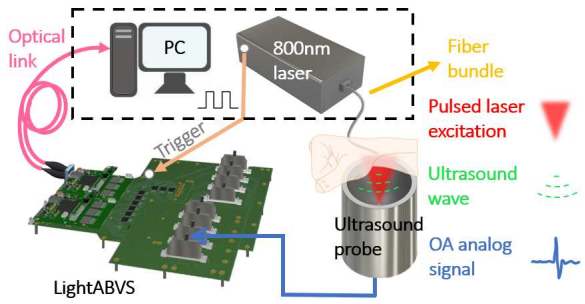

Fig. 1. Sketch of the experimental setup. An 800 nm laser is coupled to a fiber bundle and guided to an OA spherical array probe. The US signals generated via laser excitation are captured by the array and sampled with a digital acquisition system (DAQ). The acquired data are eventually sent to a host-PC for further processing.

978-1-7281-6801-2/20/$31.00 ©2020 IEEE

fulfilling the ANSI laser safety criteria [14]. The OA imaging system accommodates a spherical US array of 256 elements (Imasonic SaS, Voray, France), which collects the generated OA signals from around the region of interest. The US probe has a central frequency of 4 MHz with 100% detection bandwidth and covers 90 degrees (0.59π solid angle) [15]. Raw OA signals are collected by a data acquisition (DAQ) system with programmable duration. In this work, we used an adapted version of the compact and inexpensive *LightABVS* system (see Sect. II-B) to perform data acquisition.

For comparison, we performed measurements with a conventional DAQ system (48×48×20 cm dimensions) consisting of 512 parallel analog-to-digital converters arranged in 16 acquisition cards (Falkenstein Mikrosysteme GmbH, Taufkirchen, Germany), which was previously employed for OA imaging [8][15]. This system consumes on average 370 W of electric power.

In the first experiment, we measured the OA signal generated from light-absorbing black paramagnetic polyethylene microspheres (Cospheric LLC, California, USA) of different sizes (100-µm and 200-µm), embedded in an agar phantom. For this, the outputs of the fiber bundle and the US probe were positioned on opposite sides of the microsphere. The microsphere-based phantom was aligned with the spherical ultrasound probe such that the microsphere was located at the center of the spherical array probe. The probe and the microsphere-based phantom were immersed in a water tank to ensure a proper acoustic coupling. The laser wavelength was set to 700 nm.

In the second experiment (depicted in Fig. 1), the wrist of a healthy volunteer was imaged. For this, the output of the fiber bundle was inserted into a central aperture of the spherical array, i.e., illumination and detection were performed from the same side. The acoustic coupling was ensured by molding agar between the active detection surface and the wrist, which was further covered with ultrasound gel. The laser wavelength in this experiment was set to 800 nm, corresponding to the isosbestic point of hemoglobin. The pulse repetition rate was varied between 10 to 100 Hz for the dynamic data acquisition. The wrist was moved within the probe's ROI during the acquisition so that different blood vessels were captured.

B. The LightABVS System

The *LightABVS* system has been previously introduced for classical pulse-echo US imaging applications [16]. It is a compact (18 × 22.6 cm), software-defined platform, featuring 192-channels. Inexpensive off-the-shelf components are employed, with the signals acquired, amplified, and digitized by means of an integrated analog front-end (AFE) from Texas Instruments (AFE58JD32, power efficiency of 42 mW/channel). The sampling frequency of the AFEs is f_s = 40 MHz with 12-bit resolution, and the output interface is a JESD204B. The system is modular and is built around two Xilinx Kintex Ultrascale+ FPGAs (XCKU5P), devoted to aggregating the data coming from the AFEs and sending them to a PC (as UDP packets) for further processing. The system is software-defined, meaning that arbitrary modes of operation can be implemented simply by adapting the control software and configuring the on-board FPGAs. Furthermore, it is effectively an open-platform, giving access to the raw data. *LightABVS* supports high-frame-rate modes of operation and is equipped with two optical modules (100G FireFly from Samtec) implementing a 100G Ethernet connection to the host PC. Currently, the system can operate

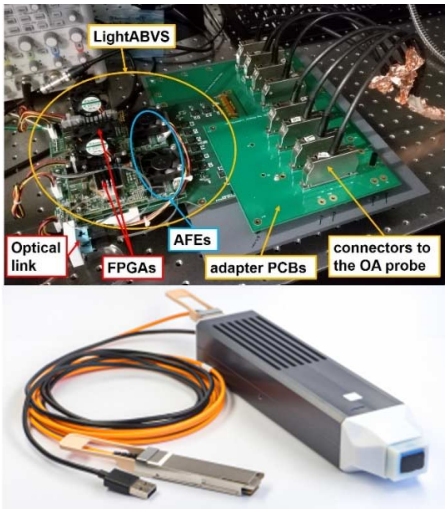

Fig. 2. Top: *LightABVS* system, connected to the OA probe via an adapter PCB. Bottom: photo of the compact *LightProbe* system [17].

up to 500 Hz, and multi-kHz frame rates can be achieved by properly adjusting (in software) the data handling approaches. Without any power management, the system consumes only 192 mW/channel. *LightABVS* can be assembled with overall cost of material and components in the 3.000 USD range.

Two adapter printed circuit boards (PCBs) were designed to connect the 192 channels of *LightABVS* to 192 out of the 256 channels of the US array (provided via 32-pins Harting connectors). The remaining channels of the probe were terminated to ground with 50 Ω resistors. Fig. 2 (top) shows a photo of *LightABVS* connected to the OA probe.

The form factor of *LightABVS* guarantees accessibility and testing during experiments. However, a much more compact version can be (and has been) developed with a partially lower performance, called *LightProbe* [17]. A photo of *LightProbe* is shown in Fig. 2 (bottom). For OA experiments, external triggering of the FPGAs was provided by the Q-switch output of the laser (Fig. 1), and the firmware of the FPGA was updated in order to be externally triggered. The signal coming from the OA probe is routed to the AFE chips and ultimately to the FPGAs, which capture the data and send them to the host PC via the optical link. For rendering each image frame, N_s = 1000 samples are captured for each channel, corresponding to an imaged region of 37.5 mm (assuming ~1500 m/s speed-of-sound in soft tissues).

III. RESULTS

As a first step, experiments with the light-absorbing microspheres were performed, serving as a validation for using the adapted version of LightABVS for OA imaging. The volumetric OA data were reconstructed using a Radon-

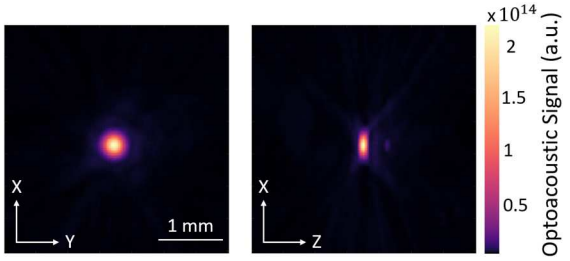

Fig. 3. OA images of a 100-µm microsphere measured with the *LightABVS* system, with 37 dB signal amplification.

transform-based algorithm [18], which involves deconvolution, band-pass filtering, and spherical back-projection steps.

Fig. 3 shows the maximum intensity projections (MIPs) of the volumetric OA reconstructions of the 100-µm microsphere along the z and y directions. The selected 192 channels provide sufficiently dense spatial sampling for accurate reconstruction of the sphere. Images generated with the conventional DAQ system (not shown) are fully consistent with the results obtained with LightABVS, attaining similar image quality and SNR. The achievable resolution is mainly determined by the transducer response. Following the approach of [19], we estimate it by extracting the full-width half-maximum of the image profile along a cross-section, and then subtracting the diameter of the microsphere. The extracted resolution is approximately 200 µm.

Table I reports the mean signal-to-noise ratio (SNR, average over all channels) for two different amplification levels of *LightABVS* (namely, 22 dB and 37 dB) and, as a comparison, for the conventional DAQ system with 40 dB amplification. The SNR is estimated from the time traces as a ratio between the peak-to-peak signal response and the noise floor. The first and second rows of Tab. 1 show SNR values obtained from the 100- and 200-µm microsphere measurements, respectively. SNR values are higher for the 200-µm microsphere measurement, as expected due to its stronger signal magnitude. Overall, there was no significant difference between the SNR attained with the *LightABVS* electronics versus the conventional DAQ system when acquiring the challenging low-intensity acoustic signals typical for OA imaging applications.

In the second experiment, the suitability of *LightABVS* for non-invasive hand-held imaging of living tissue was assessed. Fig. 4 shows four selective volumetric OA images of human vasculature in the wrist region at different acquisition rates, namely 10 Hz (a) and 100 Hz (b). The 3D optoacoustic data were reconstructed using the same back-projection algorithm [18]. The reconstruction volume is a $10\times10\times10$ mm^3 with a resolution of $100\times100\times100$ voxels. The images in the top and bottom panels of Figs. 4a and 4b represent maximum intensity projections (MIPs) of the volumetric reconstructions along the z and y directions, respectively. As expected, the shift in two consecutive frames in Fig. 4a acquired with a frame rate of 10 Hz is more significant as compared to the faster 100 Hz recordings (Fig. 4b).

IV. DISCUSSION AND CONCLUSION

The imaging results presented in this work demonstrate the feasibility of real-time 3D OA imaging with the compact, low-cost, and configurable *LightABVS* acquisition platform.

TABLE I. SNR comparison between different amplification levels of *LightABVS* and conventional DAQ, for the 100-µm (top row) and 200-µm microsphere (bottom row) measurements.

Microsphere	Conventional DAQ (40 dB)	LightABVS (22 dB)	LightABVS (37 dB)
100 µm	32.2 dB	31.4 dB	32.2 dB
200 µm	51.6 dB	47.2 dB	48.1 dB

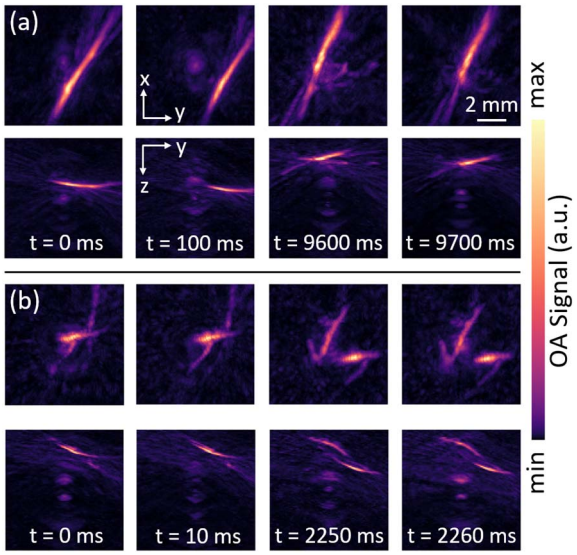

Fig. 4. Volumetric OA images (normalized to the maximum) taken from a healthy human volunteer (wrist region) using the *LightABVS* electronics. Consecutive image volumes are shown at 10 Hz (a) and 100 Hz (b) acquisition rates.

This opens new opportunities for the development of more compact and affordable hand-held OA scanners to be used in clinical applications, which is of particular importance considering the ongoing clinical translation of this modality [20]. The achieved imaging rate of 100 frames per second is currently limited by the PRF of the laser and could be significantly accelerated if other light sources are employed. For instance, laser diodes can provide per-pulse energies in the millijoule range at PRFs in the order of several kHz [21]. The transmission bandwidth of the *LightABVS* fiber optical connector is sufficient to transmit all the digitized signals when operating in this PRF range provided the software in the host computer is configured to process the received data.

Future development steps will focus on demonstrating the operability of 3D imaging at frame rates of hundreds to thousands of Hz via dense spatial tomographic sampling of the pressure signals captured by the detection array. Furthermore, real-time preview during acquisition will be implemented, starting from 3D image rendering approaches at ~50 frames per second that have been previously demonstrated using graphics processing unit (GPU) implementation of a back-projection formula [18], which is sufficient for video-rate visualization. Finally, the integration of OA and US imaging modalities is also planned as future work. In conclusion, the newly developed platform opens up promising opportunities for the development of more compact, affordable, and flexible OA imaging systems.

ACKNOWLEDGMENT

The authors thank A. Blanco Fontao and H. Gisler (ETH Zürich) for technical support. X. L. D. B. acknowledges support from the Werner und Hedy Berger-Janser Stiftung (Application No 08/2019). D. R. acknowledges support from the European Research Council under grant agreement ERC-CoG_2015_682379.

REFERENCES

[1] K. K. Shung, "Diagnostic ultrasound: Past, present, and future," J. Med. Biol. Eng., vol. 31, no. 6, pp. 371–374, 2011

[2] A. Eklund, P. Dufort, D. Forsberg, and S. M. LaConte, "Medical image processing on the GPU–Past, present and future," Med. Image Anal., vol. 17, no. 8, pp. 1073-1094, 2013

[3] M. I. Fuller, T. N. Blalock, J. A. Hossack, and W. F. Walker, "A portable, low-cost, highly integrated, 3D medical ultrasound system," IEEE Symp. Ultrason., vol. 1, pp. 38–41, 2003.

[4] L. V. Wang and J. Yao, "A practical guide to photoacoustic tomography in the life sciences," Nat. Methods, vol. 13. no.8, pp. 627-638, 2016.

[5] X. L. Deán-Ben, S. Gottschalk, B. Mc Larney, S. Shoham, and D. Razansky, "Advanced optoacoustic methods for multiscale imaging of in vivo dynamics," Chem. Soc. Rev., vol. 46, no.8, pp. 2158-2198, 2017.

[6] G. Diot, S. Metz, A. Noske, E. Liapis, B. Schroeder, S. V. Ovsepian, R. Meier, E. Rummeny and V. Ntziachristos, "Multispectral Optoacoustic Tomography (MSOT) of Human Breast Cancer," Clin. Cancer Res., vol. 23, no.22, pp. 6912-6922, 2017.

[7] A. P. Regensburger, L. M. Fonteyne, J. Jüngert, A. L. Wagner, T. Gerhalter, A. M. Nagel, R. Heiss, F. Flenkenthaler, M. Qurashi, M. F. Neurath, N. Klymiuk, E. Kemter, T. Fröhlich, M. Uder, J. Woelfle, W. Rascher, R. Trollmann, E. Wolf, M. J. Waldner and F. Knieling,"Detection of collagens by multispectral optoacoustic tomography as an imaging biomarker for Duchenne muscular dystrophy," Nat. Medicine, vol. 25, no.12, pp. 1905-1915, 2019.

[8] E. Merčep, X. L. Deán-Ben, and D. Razansky, "Combined pulse-echo ultrasound and multispectral optoacoustic tomography with a multi-segment detector array," IEEE Trans. Med. Imaging, vol. 36, no.10, pp. 2129-2137, 2017.

[9] J. Kim, S. Park, Y. Jung, S. Chang, J. Park, Y. Zhang, J. F. Lovell, and C. Kim, "Programmable real-time clinical photoacoustic and ultrasound imaging system," Sci. Rep., vol. 6, no.35137, 2016.

[10] M. Oeri, W. Bost, N. Sénégond, S. Tretbar, M. Fournelle., "Hybrid photoacoustic/ultrasound tomography for real-time finger imaging," Ultrasound Med. Biol., vol. 43, no.10, pp. 2200-2212, 2017.

[11] L. Li, L. Zhu, C. Ma, L. Lin, J. Yao, L. Wang, K. Maslov, R. Zhang, W. Chen, J. Shi and L. V. Wang, "Single-impulse panoramic photoacoustic computed tomography of small-animal whole-body dynamics at high spatiotemporal resolution," Nat. Biomed. Eng., vol. 1, no. 5, pp. 1-11, 2017.

[12] E. Merčep, J. L. Herraiz, X. L. Deán-Ben, and D. Razansky, "Transmission–reflection optoacoustic ultrasound (TROPUS) computed tomography of small animals," Light Sci. App., vol. 8, no. 1, pp. 1-12, 2019.

[13] A. Özbek, X. L. Deán-Ben, and D. Razansky, "Optoacoustic imaging at kilohertz volumetric frame rates", Optica, 5(7), pp. 857-863, 2018.

[14] American National Standards for the Safe Use of Lasers ANSI Z136.1, American Laser Institute, 2000.

[15] X. L. Deán-Ben, A. Ozbek and D. Razansky, "Volumetric Real-Time Tracking of Peripheral Human Vasculature With GPU-Accelerated Three-Dimensional Optoacoustic Tomography," IEEE Trans. Med. Imaging, vol. 32, no. 11, pp. 2050-2055, 2013.

[16] P. A. Hager, F. Kuhn Jush, M. Biele, P. M. Düppenbecker, O. Schmidt, and L. Benini, "LightABVS: A Digital Ultrasound Transducer for Multi-Modality Automated Breast Volume Scanning," IEEE International Ultrasonics Symposium, UK, October 2019.

[17] P. A. Hager and L. Benini, "LightProbe: A Digital Ultrasound Probe for Software-Defined Ultrafast Imaging," IEEE Trans. Ultrason. Ferroelectr. Freq. Control, vol. 66, no. 4, pp. 747-760, 2019.

[18] A. Ozbek, X. L. Deán-Ben, and D. Razansky "Realtime parallel back-projection algorithm for three-dimensional optoacoustic imaging devices", Proc. SPIE 8800, Opto-Acoustic Methods and Applications, 88000I, June 2013.

[19] X. L. Deán-Ben and D. Razansky, "Portable spherical array probe for volumetric real-time optoacoustic imaging at centimeter-scale depths," Opt. Express, vol. 21, no. 23, pp. 28062-28071.

[20] V. Neuschmelting, N. C. Burton, H. Lockau, A. Urich, S. Harmsen, V. Ntziachristos and M. F. Kircher, "Performance of a multispectral optoacoustic tomography (MSOT) system equipped with 2D vs. 3D hand-held probes for potential clinical translation," Photoacoustics, vol. 4, no. 1, pp. 1-10, 2016.

[21] K. Daoudi, P. J. Van Den Berg, O. Rabot, A. Kohl, S. Tisserand, P. Brands, and W. Steenbergen, "Hand-held probe integrating laser diode and ultrasound transducer array for ultrasound/photoacoustic dual modality imaging," Opt. Express, vol. 22, no. 21, pp. 26365-26374, 2014.